A transient regime for transforming thermal convection: Cloaking, concentrating, and rotating creeping flow and heat flux

Gaole Dai, and Jiping Huang

Citation: Journal of Applied Physics **124**, 235103 (2018); doi: 10.1063/1.5051524
View online: https://doi.org/10.1063/1.5051524
View Table of Contents: http://aip.scitation.org/toc/jap/124/23
Published by the American Institute of Physics

A transient regime for transforming thermal convection: Cloaking, concentrating, and rotating creeping flow and heat flux

Gaole Dai and Jiping Huang[a)]
Department of Physics, State Key Laboratory of Surface Physics, and Key Laboratory of Micro and Nano Photonic Structures (MOE), Fudan University, Shanghai 200433, China and Collaborative Innovation Center of Advanced Microstructures, Nanjing 210093, China

(Received 9 August 2018; accepted 20 November 2018; published online 17 December 2018)

By treating a set of equations governing transient heat and mass transfer simultaneously, here we develop the transformation theory for thermal convection with unsteady creeping flow in porous media, whose steady counterpart has been previously studied. We find that the transformation theory can still be valid when the temperature, density, and velocity of fluids vary with time. As applications, we design thermal cloaks, concentrators, and rotators at transient states examined by finite-element simulations, which can be used to control the magnitude or direction of heat flux in convection. Also, we discuss both the effects of natural or mixed convection and the differences between steady and unsteady states. This work develops a theory for dynamically controlling the flow of heat associated with thermal convection. *Published by AIP Publishing.*
https://doi.org/10.1063/1.5051524

I. INTRODUCTION

Heat transfer, via thermal conduction, radiation, or convection, is a ubiquitous phenomenon which has arisen continuing concern on how to control it for promoting energy efficiency in production and daily life. By now, most researchers have focused on manipulating conduction and radiation, including thermal cloaks/concentrators/rotators/camouflage/imitator,[1–20] thermocrystals,[21–23] nanophononic metamaterials,[24–27] and radiative cooling.[28–34] In the mean time, controlling convection has been rarely studied.

Convection is usually the dominant mechanism of heat transfer in moving fluids, where heat flux is driven by both bulk flow and temperature spatial-gradient (governed by a convection-diffusion equation). So, heat and mass transfer are actually coupled with each other. As a result, when managing heat transfer by convection, the methods dealing with the convection-diffusion equation[35,36] and fluid movement[37–40] should be combined together. In the light of transforming the convection-diffusion equation,[35,36] we established the theory for transforming thermal convection in porous media for steady cases.[41] To get a set of equations keeping their forms invariant in different coordinate systems, we considered the convection-diffusion equation, the equation of continuity, and Darcy's law simultaneously. By transforming the effective thermal conductivity and permeability, we successfully designed a cloak of invisibility in the fields of both temperature and velocity and a concentrator that can enlarge the heat flux in a specific area. However, an unsteady state (which means that some physical quantities change with time slightly or intensely) is a more general case, and its new physics can be expected due to the difference between unsteady and steady cases.

In this work, we develop the transformation theory for unsteady thermal convection of creeping flow in porous media based on the model raised in Ref. 41, where the temperature, velocity, and material density can all be non-constant during the process of heat and mass transfer. Then, we also confirm the theoretical designs of convection cloaks, concentrators, and rotators in such unsteady states by using finite-element simulations on the basis of commercial software COMSOL Multiphysics.[42]

II. THEORY

Transformation theory, first proposed in optics,[43,44] has been widely used to design thermal metamaterials[1–6,9–19]

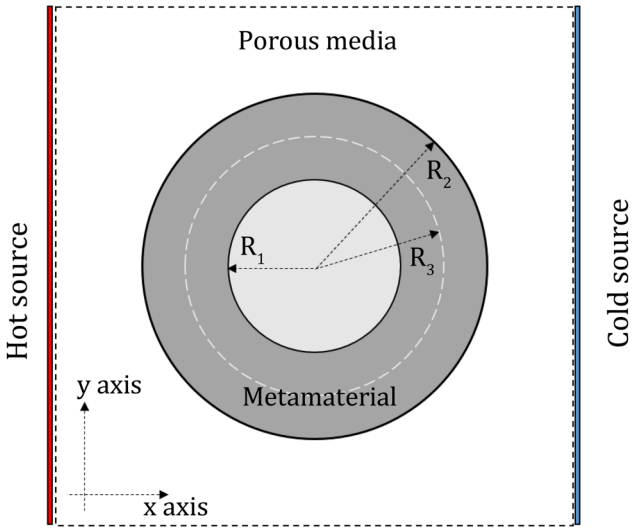

FIG. 1. Schematic design for a cloak, concentrator, or rotator in thermal convection. The ring-shaped area in gray is made of thermal metamaterial with the function of cloaking, concentrating, or rotating for corresponding coordinate transformations. The white dotted lines form a circle with a radius of R_3, representing the auxiliary parameter in designing concentrators.

[a)]Electronic address: jphuang@fudan.edu.cn

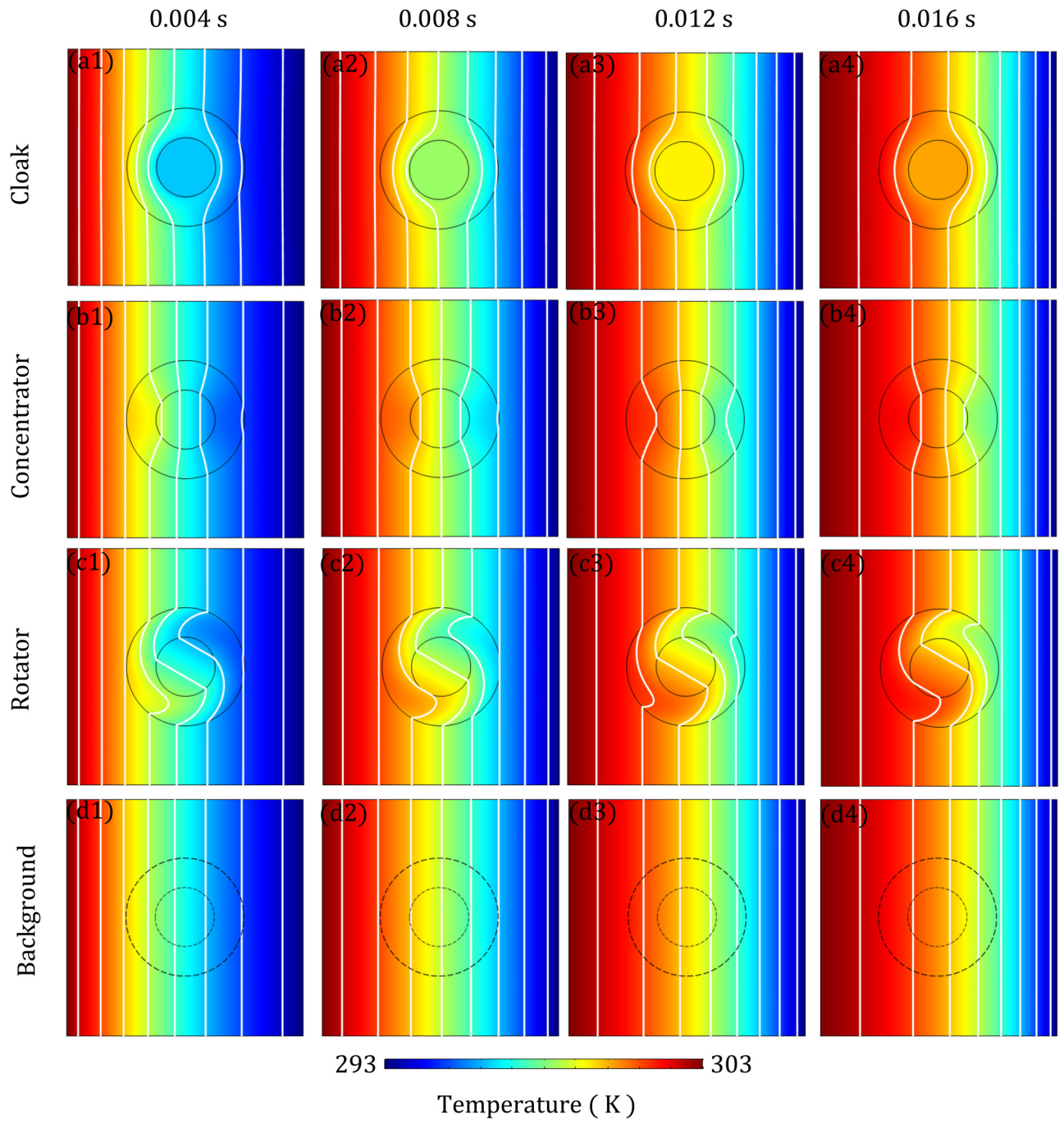

FIG. 2. Simulation results of temperature distribution for forced convection. The white lines represent isotherms. The first row (a1)–(a4) shows the temperature distributions of a thermal cloak at time $t = 0.004\,\mathrm{s}$, $t = 0.008\,\mathrm{s}$, $t = 0.012\,\mathrm{s}$, and $t = 0.016\,\mathrm{s}$. Similarly, (b1)–(b4) show those of a thermal concentrator, (c1)–(c4) show those of a thermal rotator, and (d1)–(d4) show those of the background.

based on the form-invariance of governing equation under arbitrary coordinate transformations. By changing the properties of materials, we can stretch, condense, or bend the physical field as if the space itself was stretched, condensed, or bended. Here, we expand the transformation theory for transient thermal convection in porous media. Firstly, for Darcy's law, we can modify it as[45–47]

$$\tau\frac{\partial\vec{v}}{\partial t}+\vec{v}=-\frac{\beta}{\eta}\nabla p, \tag{1}$$

where τ represents a characteristic time for varying velocity $\vec{v}$ with time t, β is the permeability of porous media, and η is the dynamic viscosity. In most cases, the relaxation process is very fast in porous media, and then $\tau\frac{\partial\vec{v}}{\partial t}$ is quite small.[47] Therefore, we can neglect this term and still use the steady Darcy regime. Also, the equation of continuity can be rewritten as[48]

$$\frac{\partial(\phi\rho_f)}{\partial t}+\nabla\cdot(\rho_f\vec{v})=0, \tag{2}$$

where ρ_f is the density of the fluid material and ϕ is the porosity. Then, the heat transfer of incompressible flow in

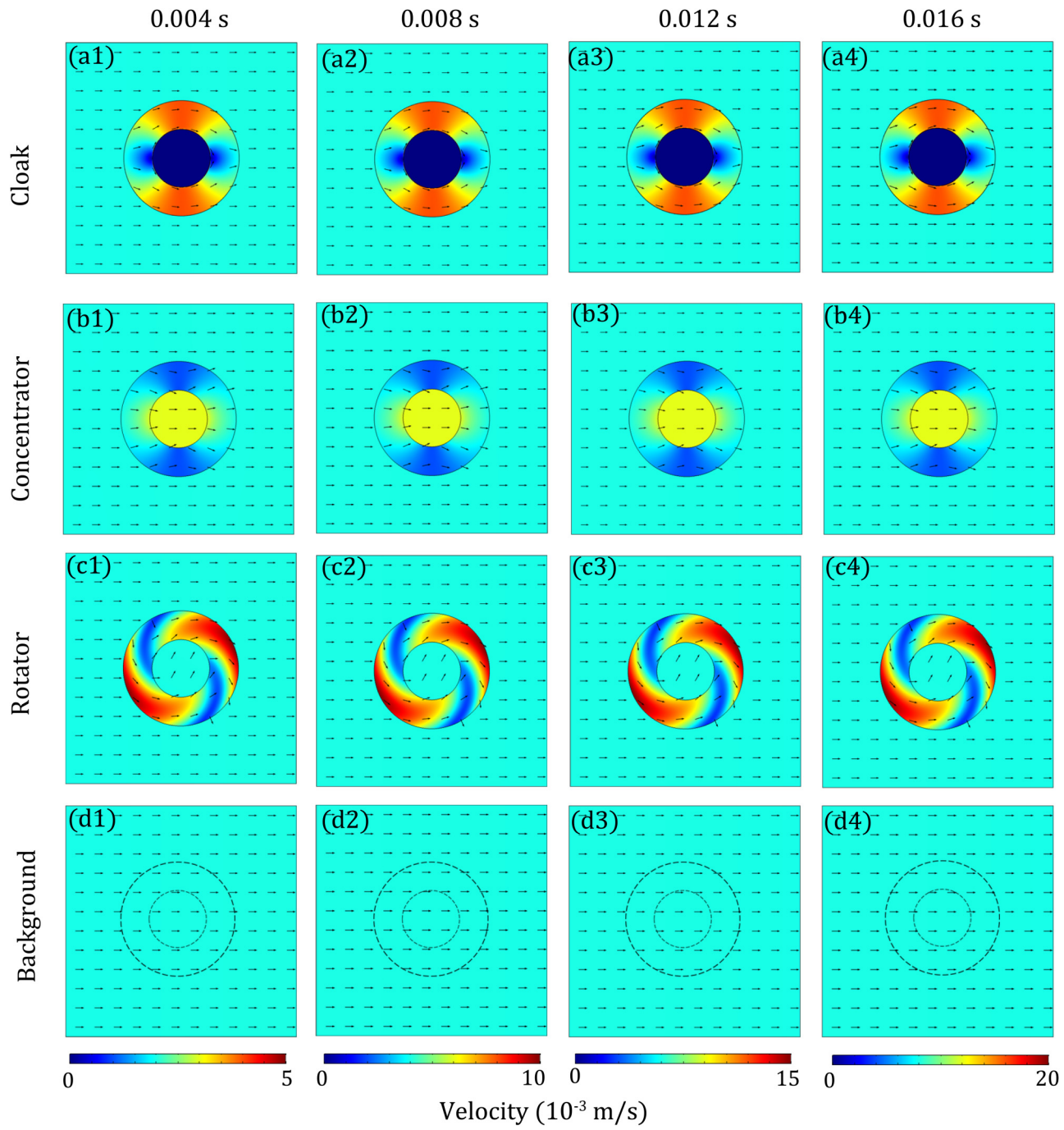

FIG. 3. Simulation results of velocity distribution for forced convection. The color surface represents the value of speed, and the black arrows represent the directions of velocities. Again, row (a1)–(a4) shows the velocity distributions of a thermal cloak at time $t = 0.004$ s, $t = 0.008$ s, $t = 0.012$ s, and $t = 0.016$ s. (b1)–(b4), (c1)–(c4), and (d1)–(d4) show those of a concentrator, a rotator, and the background, respectively.

saturated porous media is governed by[49,50]

$$\frac{\partial(\rho C)_m T}{\partial t} + \nabla \cdot (\rho_f C_f \vec{v} T) = \nabla \cdot (\kappa_m \nabla T), \tag{3}$$

where T is temperature and ρ_s is the density of solid in porous media. Here, C_f and C_s are, respectively, the specific heat of fluid and solid material in porous media. The effective product of density and specific heat of the whole porous media can be given by the average-volume method:[50]

$$(\rho C)_m = (1 - \phi)(\rho_s C_s) + \phi(\rho_f C_f). \tag{4}$$

Similarly, the effective heat conductivity κ_m can also be the summation of κ_f (for fluids) and κ_s (for solids) according to the mean-volume method:

$$\kappa_m = (1 - \phi)\kappa_s + \phi\kappa_f. \tag{5}$$

We notice that Eq. (3) is just the unsteady convection-diffusion equation whose form-invariance under coordinate transformations has been proved.[35,36] What's more, the

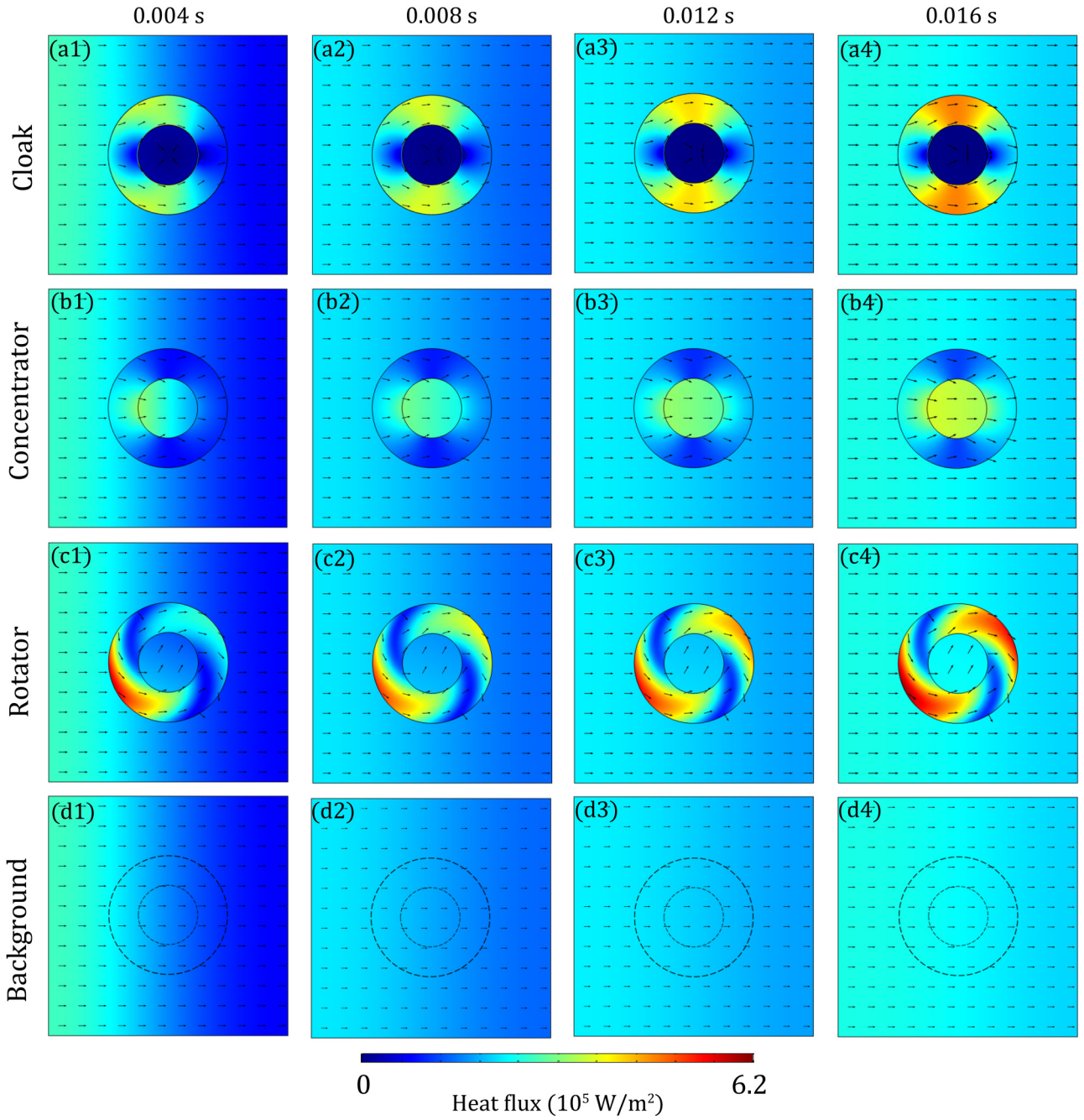

FIG. 4. Simulation results of heat flux distribution for forced convection. The value of heat flux is displayed by the color surface, and the black arrows here represent the directions of heat flux. Row (a1)–(a4) shows the heat flux distribution of a thermal cloak at time $t = 0.004$ s, $t = 0.008$ s, $t = 0.012$ s, and $t = 0.016$ s. (b1)–(b4), (c1)–(c4), and (d1)–(d4) are for the concentrator, rotator, and background, respectively.

substitution of Eq. (2) into Eq. (3) yields

$$(\rho C)_m \frac{\partial T}{\partial t} + \rho_f C_f (\vec{v} \cdot \nabla T) = \nabla \cdot (\kappa_m \nabla T). \tag{6}$$

Since Eq. (2) is an unsteady diffusion equation, it is easy to conclude that all the equations for unsteady heat and mass transfer in porous media can meet the requirement of transformation theory just like the steady cases.[41] For both steady and unsteady cases, the transformation matrix for a homogeneous space is $\frac{\mathbf{J}\mathbf{J}^\top}{\det \mathbf{J}}$, where $\mathbf{J}$ is the Jacobian matrix from the transformed coordinate to the original one. Still, we should transform the permeability and heat conductivity as $\beta' = \frac{\mathbf{J}\beta\mathbf{J}^\top}{\det \mathbf{J}}$ and $\kappa'_m = \frac{\mathbf{J}\kappa_m\mathbf{J}^\top}{\det \mathbf{J}}$. The difference is that, for unsteady cases, we must also transform the porosity and the product of density and specific heat as

$$\begin{cases} \phi' = \frac{\phi}{\det \mathbf{J}}, \\ (\rho_f C_f)' = \rho_f C_f, \\ (\rho_s C_s)' = \frac{1-\phi}{\det \mathbf{J}-\phi} \rho_s C_s. \end{cases} \tag{7}$$

By this way, we can keep the properties of fluid unchanged after transformation and only construct solid metamaterials as we need. We should also mention that ρ_f is no longer a constant as it has a relationship with temperature changing with

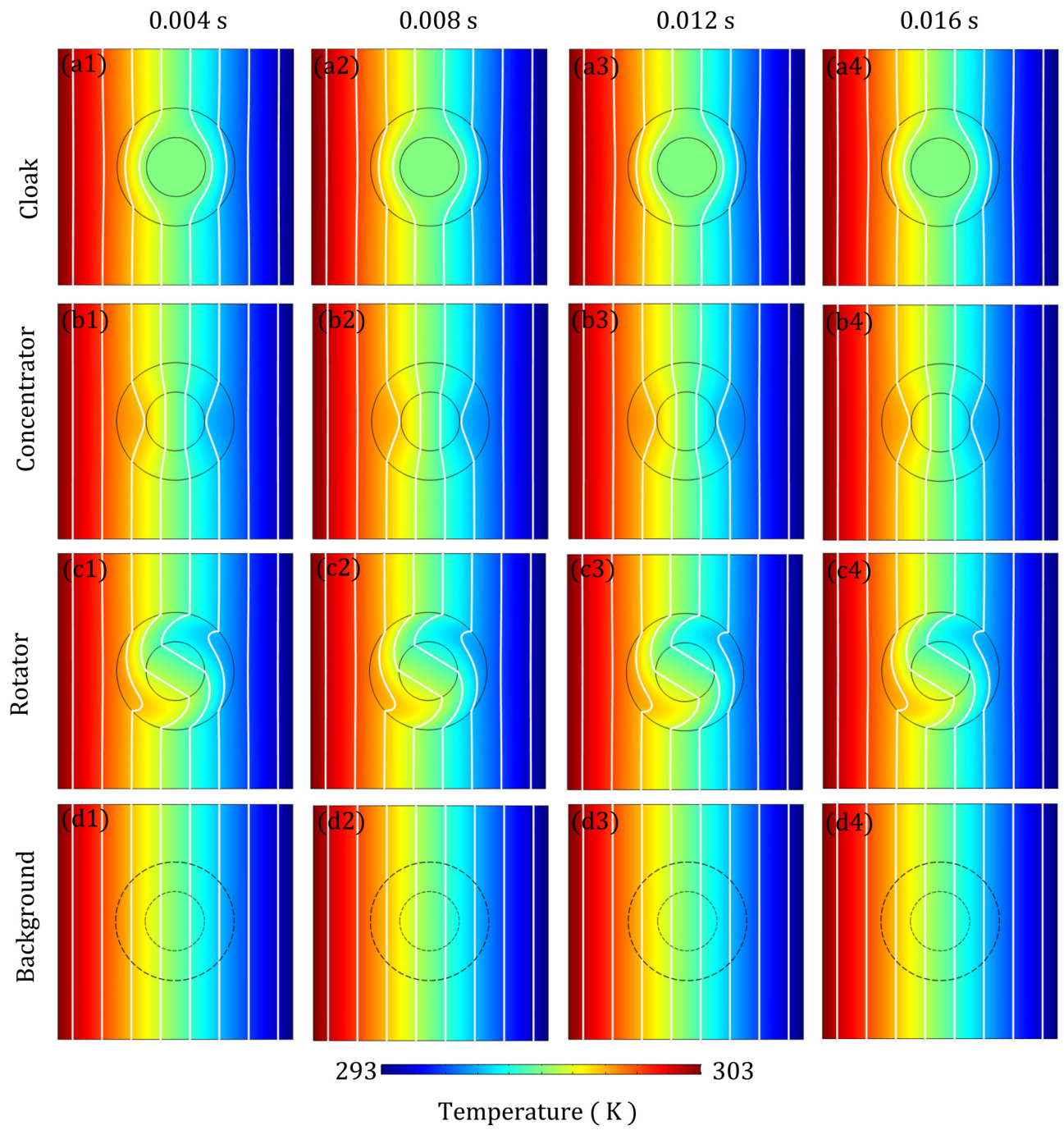

FIG. 5. Same as Fig. 2, but for another working fluid with a smaller Prandtl number.

time. For simplicity, we assume that

$$\rho = \rho_0[1 - \gamma(T - T_0)], \tag{8}$$

where $\gamma = (\frac{\partial \rho}{\partial T})_p/\rho$ denotes the volume expansion ratio at constant pressure. Without loss of generality, we set $\gamma > 0$. Finally, we can write the set of transformed equations:

$$\begin{cases} \vec{v}' = -\frac{\beta'}{\eta}\nabla p, \\ \frac{\partial(\phi'\rho_f)}{\partial t} + \nabla \cdot (\rho_f \vec{v}') = 0, \\ (\rho C)'_m \frac{\partial T}{\partial t} + \rho_f C_f(\vec{v}' \cdot \nabla T) = \nabla \cdot (\kappa'_m \nabla T), \end{cases} \tag{9}$$

where the transformed velocity $\vec{v}'$ equals $\mathbf{J}^\top \vec{v}/\det \mathbf{J}$[35,36,41] and $(\rho C)'_m = (1 - \phi')(\rho_s C_s)' + \phi'(\rho_f C_f)$.

III. CONVECTION CLOAK, CONCENTRATOR, AND ROTATOR

Generally, there may be two aspects for manipulating heat flux, namely, controlling area (volume) or direction. For heat conduction, some novel functional devices have been successfully designed, such as thermal cloaks[1–10,14] (reducing the area of heat flux in a given region), thermal concentrators (enhancing the area of heat flux in a given region),[4,5,17] and thermal rotators (changing the direction of

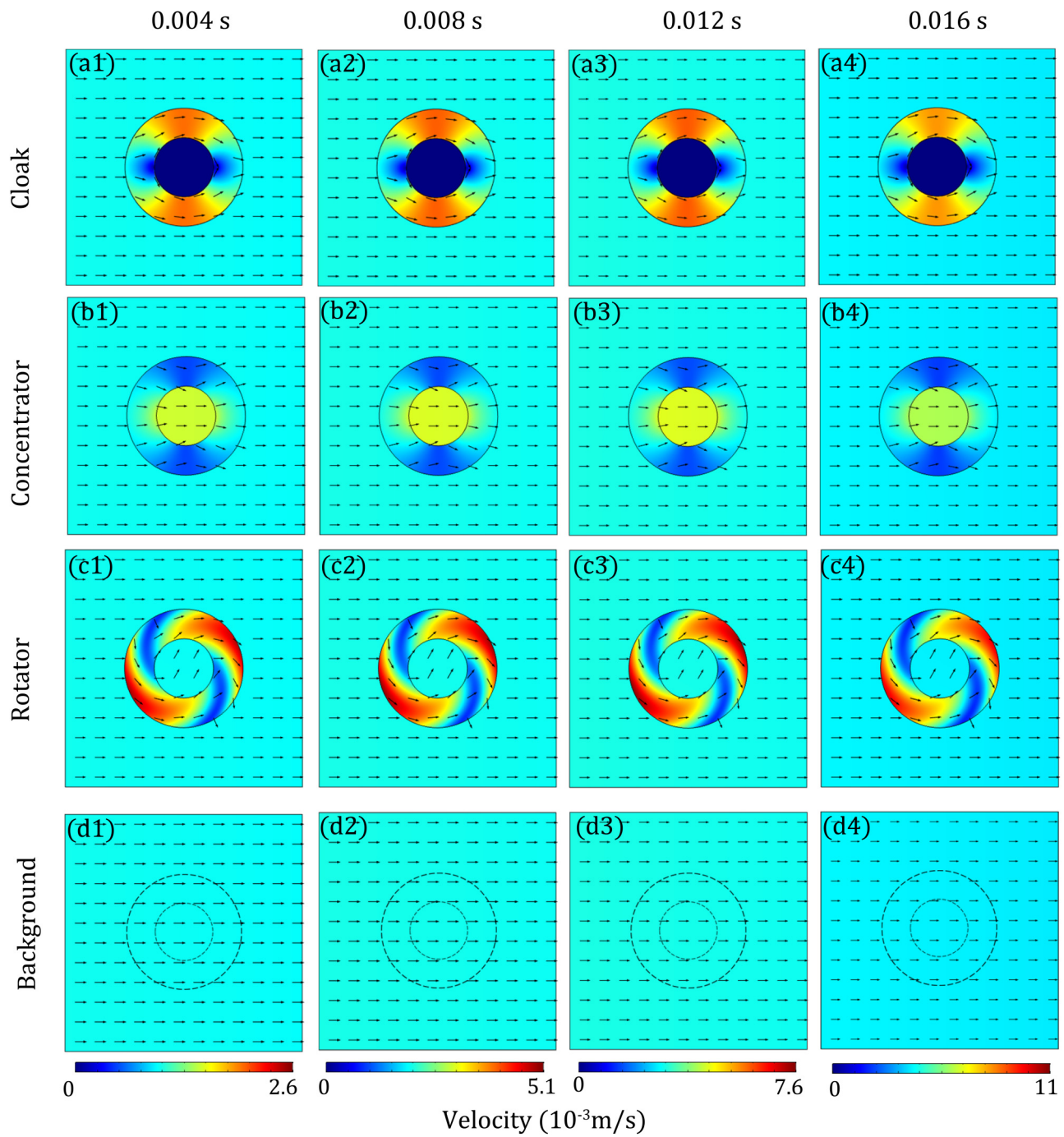

FIG. 6. Same as Fig. 3, but for another working fluid with a smaller Prandtl number.

heat flux).[5] Also, a cloak and a concentrator for steady thermal convection have been theoretically designed[41] while the rotator has not. Here, we try to realize the same effects in transient thermal convection. For simplicity, we set our models in a two-dimensional space and consider circular cloaks/concentrators/rotators (Fig. 1).

Cloak. The familiar geometrical transformation[43]

$$\begin{cases} r' = R_1 + \frac{R_2 - R_1}{R_2} r, \ 0 < r < R_2, \\ \theta' = \theta \end{cases} \tag{10}$$

is used to protect the outside region $r' > R_1$ from being disturbed by objects placed in $0 < r' < R_1$. The corresponding Jacobian matrix is

$$\mathbf{J} = \begin{pmatrix} \cos\theta & -r'\sin\theta \\ \sin\theta & r'\cos\theta \end{pmatrix} \begin{pmatrix} \frac{R_2 - R_1}{R_2} & 0 \\ 0 & 1 \end{pmatrix} \begin{pmatrix} \cos\theta & \sin\theta \\ -\frac{\sin\theta}{r} & \frac{\cos\theta}{r} \end{pmatrix}, \tag{11}$$

and it is easy to see

$$\det \mathbf{J} = \frac{R_2 - R_1}{R_2} \frac{r'}{r}. \tag{12}$$

Concentrator. Consider the transformation adopted in

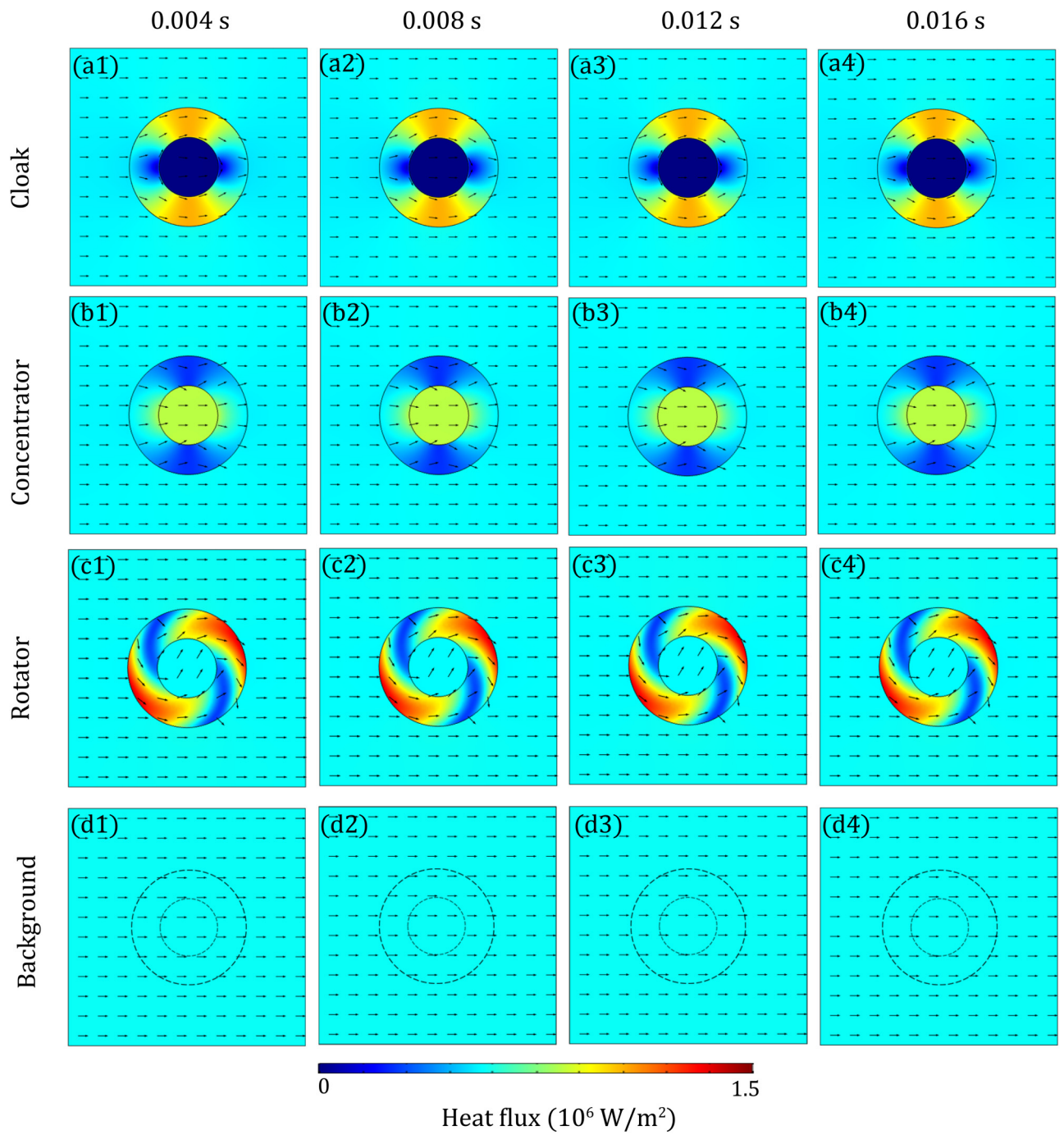

FIG. 7. Same as Fig. 4, but for another working fluid with a smaller Prandtl number.

Ref. 51

$$\begin{cases} r' = \frac{R_1}{R_3} r, \; r < R_3, \\ r' = \frac{R_1 - R_3}{R_2 - R_3} R_2 + \frac{R_2 - R_1}{R_2 - R_3} r, \quad R_3 < r < R_2, \end{cases} \tag{13}$$

which squeezes region $0 < r < R_3$ to $r' < R_1$ and stretching region $R_3 < r < R_3$ to $R_1 < r' < R_2$. We can expect physical quantities to be enlarged in the squeezed region. The corresponding Jacobian matrix is

$$\mathbf{J}_1 = \begin{pmatrix} \frac{R_1}{R_3} & 0 \\ 0 & \frac{R_1}{R_3} \end{pmatrix}, \tag{14}$$

for region $r' < R_1$. So, the determinant is

$$\det \mathbf{J}_1 = \left(\frac{R_1}{R_3} \right)^2. \tag{15}$$

Also, for region $R_1 < r' < R_2$, we have

$$\mathbf{J}_2 = \begin{pmatrix} \cos\theta & -r' \sin\theta \\ \sin\theta & r' \cos\theta \end{pmatrix} \begin{pmatrix} \frac{R_2 - R_1}{R_2 - R_3} & 0 \\ 0 & 1 \end{pmatrix} \begin{pmatrix} \cos\theta & \sin\theta \\ -\frac{\sin\theta}{r} & \frac{\cos\theta}{r} \end{pmatrix}, \tag{16}$$

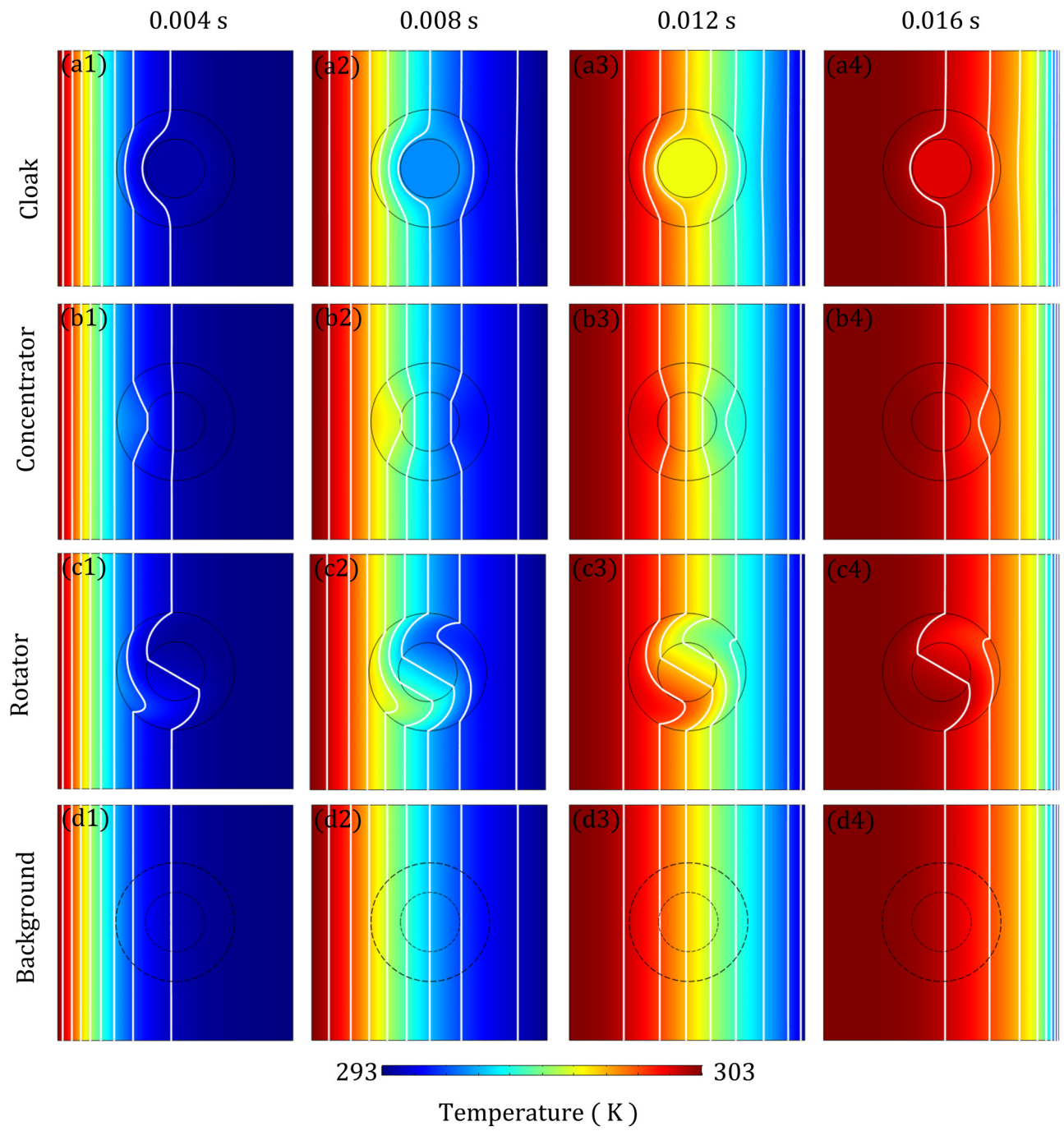

FIG. 8. Same as Fig. 2, but for a fluid whose specific heat is ten times more than that in Fig. 2.

and the determinant is

$$\det \mathbf{J}_2 = \frac{R_2 - R_1}{R_2 - R_3}\frac{r'}{r}. \tag{17}$$

Rotator. In addition, changing the direction of heat flux is also a useful way for guiding heat flow at will. Here, we focus on the continuous transformation of direction, rotation, which can be realized by a rotator. To design a rotator for heat transfer, we can consider a transformation proposed in Ref. 52,

$$\begin{cases} \theta' = \theta + \theta_0, & r < R_1, \\ \theta' = ar + b, & R_1 < r < R_2, \end{cases} \tag{18}$$

where $a = \frac{\theta_0}{R_1 - R_2}$, $b = \theta + \frac{R_2}{R_2 - R_1}\theta_0$, and $R_1 < r < R_2$. The transformation above means that region $r < R_1$ is rotated by an angle of θ_0, while in region $R_1 < r < R_2$, the rotation angle gradually decreases from θ_0 to zero as r is reduced. Again, the transformation matrix is different in these two regions. For region $r < R_1$, the Jacobian matrix is expressed as

$$\mathbf{J}_1 = \begin{pmatrix} \cos\theta_0 & -\sin\theta_0 \\ \sin\theta_0 & \cos\theta_0 \end{pmatrix} \tag{19}$$

by which we can expect the velocity and heat flux to be rotated by an angle of θ_0. What's more, we have an identity

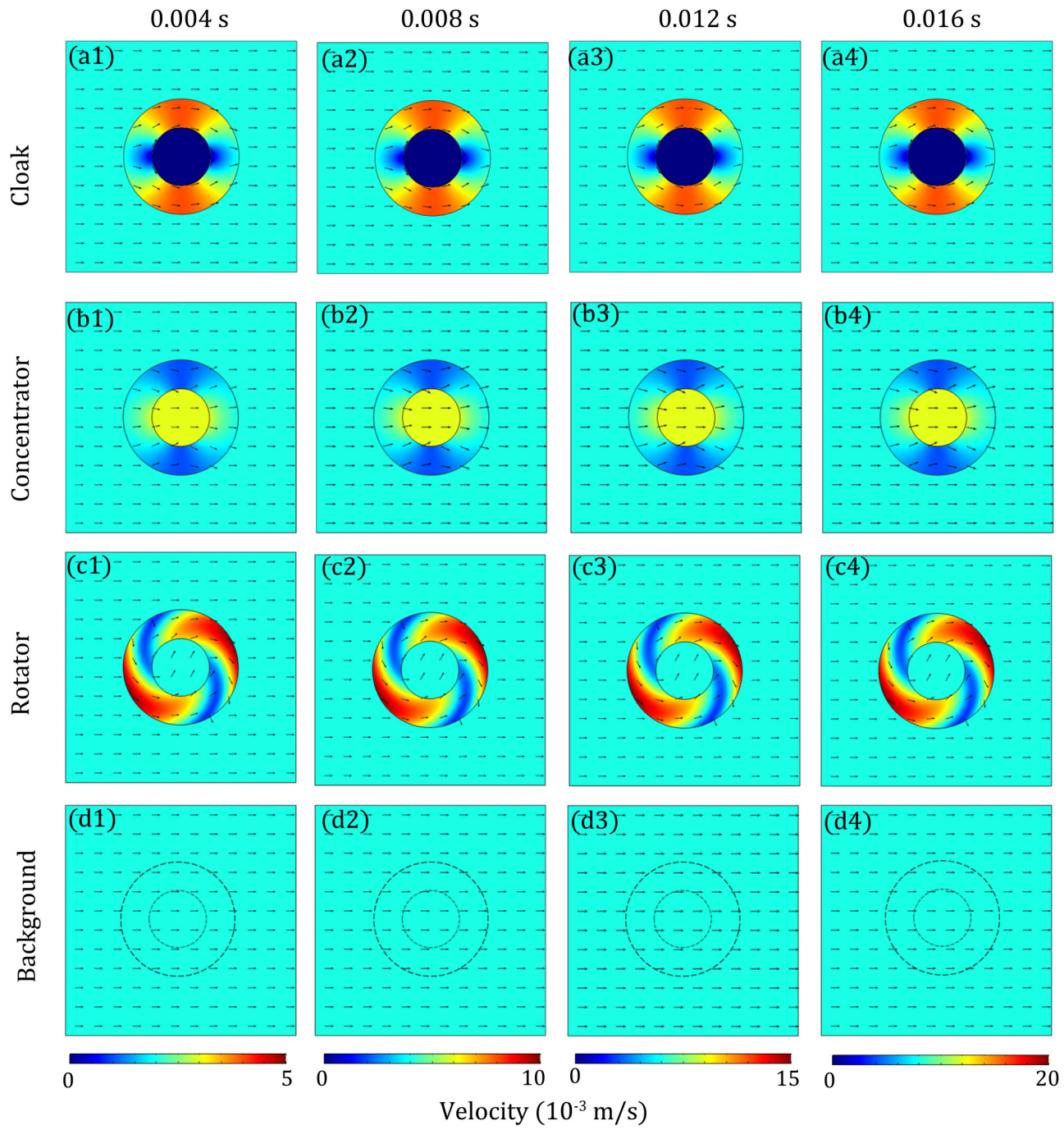

FIG. 9. Same as Fig. 3, but for a fluid whose specific heat is ten times more than that in Fig. 3.

transformation matrix as

$$\frac{\mathbf{J}_1\mathbf{J}_1^{\top}}{\det \mathbf{J}_1} == \begin{pmatrix} 1 & 0 \\ 0 & 1 \end{pmatrix}, \tag{20}$$

so in this region, we do not need to do any transformation for material properties. For region $R_1 < r < R_2$, we can also obtain a unitary Jacobian matrix as

$$\mathbf{J}_2 = \begin{pmatrix} \cos\theta' & -r\sin\theta' \\ \sin\theta' & r\cos\theta' \end{pmatrix} \begin{pmatrix} 1 & 0 \\ \alpha & 1 \end{pmatrix} \begin{pmatrix} \cos\theta & \sin\theta \\ -\frac{\sin\theta}{r} & \frac{\cos\theta}{r} \end{pmatrix}. \tag{21}$$

Simulation. To examine our theory, the commercial software COMSOL Multiphysics[42] is used to apply finite-element simulations. The whole region is restricted in a square with $-4\times10^{-5}\,\mathrm{m} \le x \le 4\times10^{-5}\,\mathrm{m}$ and $-4\times10^{-5}\,\mathrm{m} \le y \le 4\times10^{-5}\,\mathrm{m}$. For the thermal cloak, concentrator, and rotator, we all set $R_2 = 2R_1 = 2\times10^{-5}\,\mathrm{m}$. We take $R_3 = 1.5\times10^{-5}\,\mathrm{m}$ for a concentrator. In addition, the angle of rotation is $\theta_0 = \pi/3$ for a rotator. A hot source of 303 K is put on the left side of the square, and a cold source of 293 K is put on the right side. The initial temperature on the whole region is 293 K. In the $-x$ direction, we add a time-dependent pressure difference as $\Delta p = 40\,000t\,\mathrm{Pa/s}$ (which means the initial pressure difference is zero) to generate unsteady forced

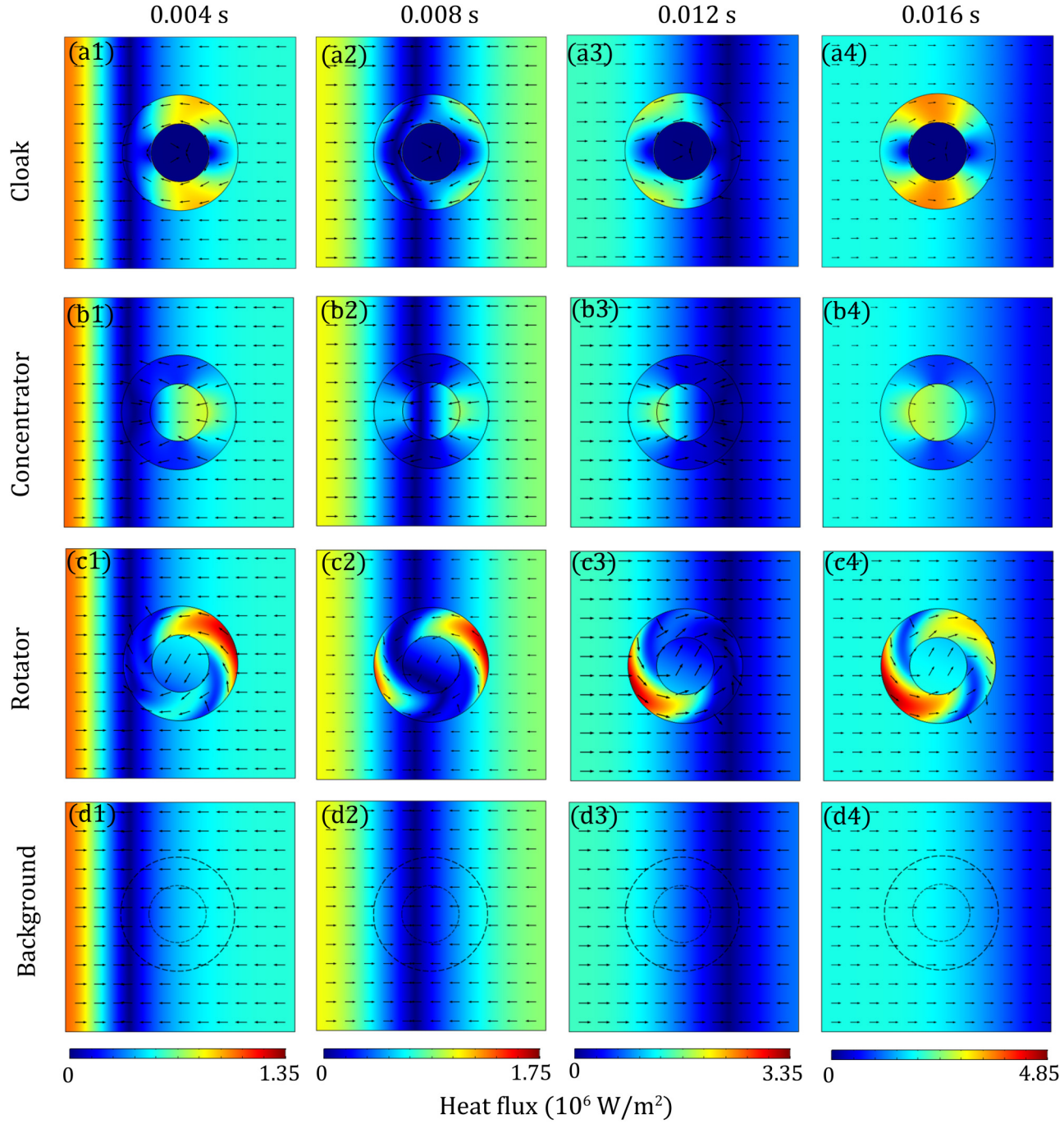

FIG. 10. Same as Fig. 4, but for a fluid whose specific heat is ten times more than that in Fig. 4.

convection and the two horizontal boundaries are set to be no-flux condition. The material parameters in background are taken as $C_f = 5 \times 10^3\,\mathrm{J/(kg\,K)}$, $\kappa_f = 1\,\mathrm{W/(m\,K)}$, $\rho_s = 500\,\mathrm{kg/m^3}$, $C_{p,s} = 500\,\mathrm{J/(kg\,K)}$, $\kappa_s = 5\,\mathrm{W/(m\,K)}$, $\phi = 0.9$, $\eta = 10^{-3}\,\mathrm{Pa\,s}$, and $\beta = 10^{-12}\,\mathrm{m^2}$. The relationship between density and temperature is $\rho_f = (1300 - T)$ with the unit of $\mathrm{kg/(K\,m^3)}$. In addition, for a thermal cloak, the object placed in the inner circle which is expected to be cloaked has a density of $10^4\,\mathrm{kg/m^3}$, a specific heat of $5 \times 10^3\,\mathrm{J/(kg\,K)}$, and a thermal conductivity of $200\,\mathrm{W/(m\,K)}$. To avoid the non-convergence in simulation of velocities due to infinite permeability, we add a restriction that the permeability of metamaterials is no more than 100 times the untransformed one. The numerical results of temperature distribution are shown in Fig. 2. What's more, Fig. 3 illustrates the velocity distribution and Fig. 4 is for the thermal flux distribution.

In addition, to see the influence of the choice of working fluid in forced convection, we do another simulation where the Prandtl number is 0.67 (similar to air), while the number takes 5 in the first simulation. The parameters of new working fluid are $\rho_f = [2.4 - 0.004 \times T/(\mathrm{K})]\,\mathrm{kg/m^3}$, $C_f = 1 \times 10^3\,\mathrm{J/(kg\,K)}$, $\kappa_f = 0.03\,\mathrm{W/(m\,K)}$, $\phi = 0.1$, $\eta = 2 \times 10^{-5}\,\mathrm{Pa\,s}$, and $\beta = 10^{-14}\,\mathrm{m^2}$. Other conditions are all the

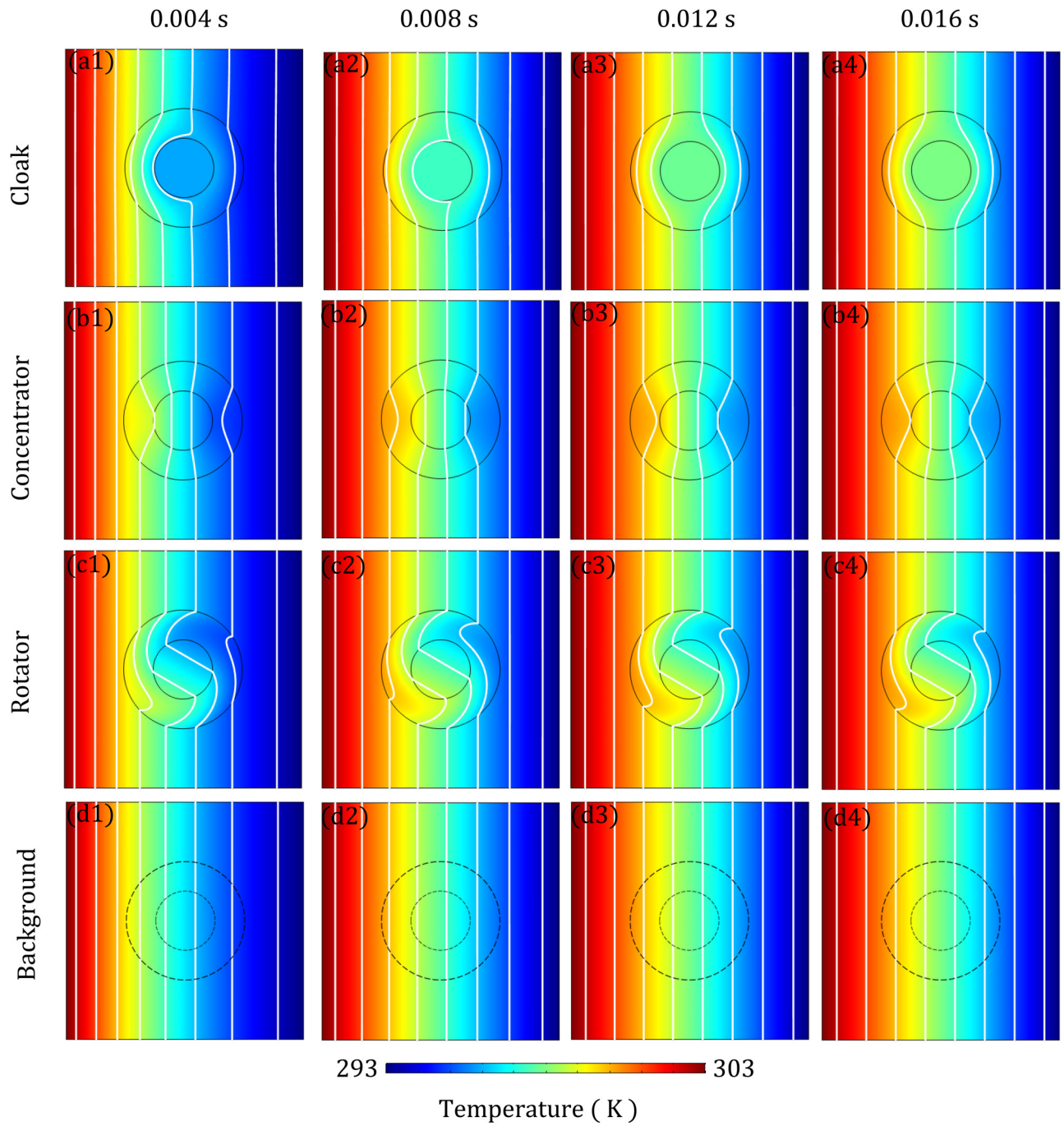

FIG. 11. Same as Fig. 2, but for natural convection.

same as the first simulation. The simulation results are shown in Figs. 5–7.

So far, we have not taken into account natural convection in our model, where the flow is driven by density difference in the field of gravity. When considering the effect of buoyancy, we should add gravitational acceleration $\vec{g}$ in Darcy's law as

$$\vec{v} = -\frac{\beta}{\eta}(\nabla p - \rho_f \vec{g}). \tag{22}$$

Then it seems quite difficult to transform $\vec{g}$ for completely satisfying the requirement of form-invariance. However, we can still evaluate the accuracy of the cloak, the concentrator, and the rotator when taking $\vec{g}$ into account. Here, $\vec{g}$ is directed along the $-y$ direction and no pressure difference is put on any boundary with no-flux condition set on the two vertical boundaries. We show the simulation result of temperature, velocity, and heat flux in Figs. 11–13, respectively, which illustrates the corresponding distributions for the cloak, concentrator, rotator and background. The material parameters are all the same as the first simulation of forced convection.

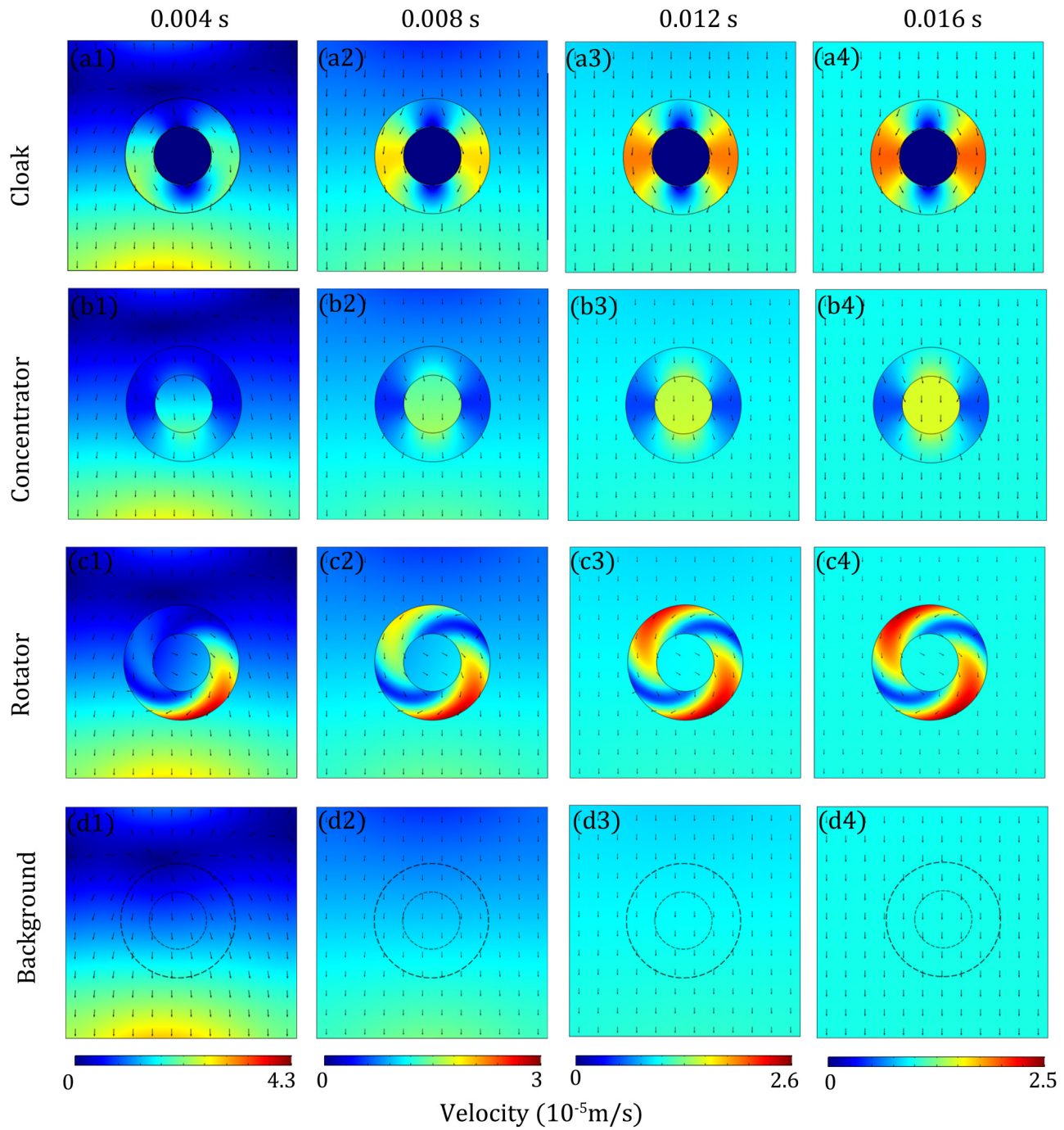

FIG. 12. Same as Fig. 3, but for natural convection.

IV. DISCUSSION AND CONCLUSION

First, we look at Fig. 2. For the coming comparison, the last row [Figs. 2(d1)–2(d4)] represents the results of the background, where the isotherms can be seen as straight lines. Comparing the first row [Figs. 2(a1)–2(a4)] with the last row [Figs. 2(d1)–2(d4)], we can see the temperatures outside the shell of metamaterial are almost undistinguishable between the cloak and background at all times. The same conclusion can be made for concentrators and rotators. For a thermal cloak, the isotherms do not cross over the core, which indicates a zero temperature gradient in this core. For a thermal concentrator, we can see from Figs. 2(b1)–2(b4) that the isotherms are more dense in the core so we can get an enlarged temperature gradient. According to Figs. 2(c1)–2(c4), the isotherms are smoothly rotated in the shell of metamaterials and finally rotated by an angle of $\pi/3$ in the core. We also show the details of the velocity in Fig. 3 and heat flux in Fig. 4. The maximum Reynolds number (for the time up to $t = 0.016$ s) is 0.16 as the background characteristic speed is approximately 0.008 m/s. In this case, Darcy's law can be applied. Similarly, the effects of cloaking, concentrating, and rotating fluid flow (or thermal flux) can be seen from Fig. 3 (or Fig. 4).

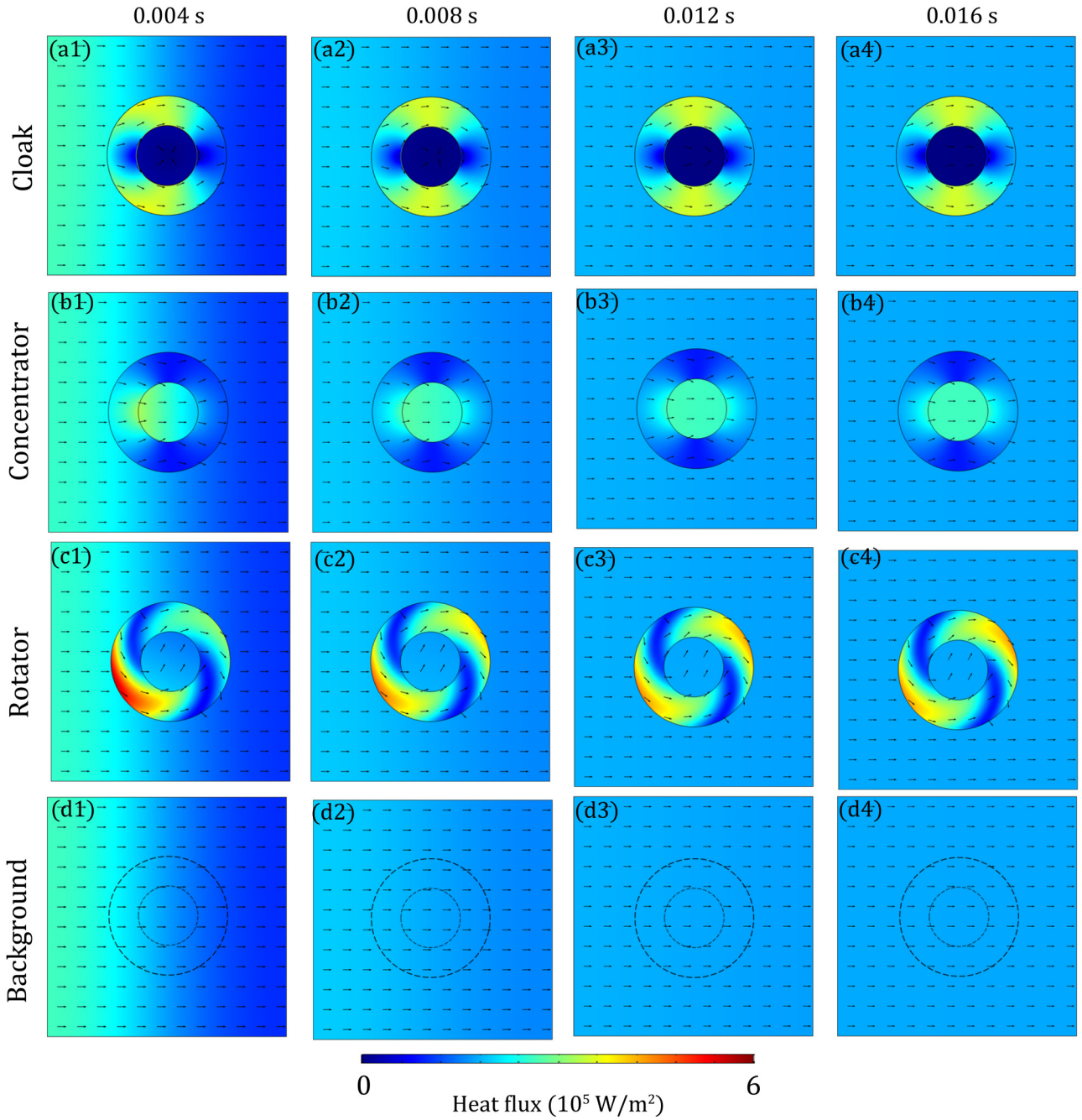

FIG. 13. Same as Fig. 4, but for natural convection.

Figures 5–7 show the temperature, velocity, and heat flux distributions, respectively, for the second working fluid in forced convection. As we expect, the effects of cloaking, concentrating, and rotating remain valid. In addition, Fig. 7 indicates that heat flux in the system quickly become stable and the patterns in Fig. 5 are similar to those for steady heat conduction. Generally, a small Prandtl number Pr means the thermal diffusion or conduction dominates rather than fluid advection. In fact, based on Eq. (3), we might use an adjusted Prandtl number $\frac{C_f\eta}{\kappa_m}$ for flow in porous media instead of $\frac{C_f\eta}{\kappa_f}$, which is 3.57 and 4.44×10^{-3} for the two working fluids. If there existed a kind of fluid whose specific heat C_f is 10 times more than the fluid we used in the first simulation while all other properties are the same, the (adjusted) Pr also increases tenfold. Again, we draw the temperature, velocity, and heat flux distributions in Figs. 8–10, respectively, for this fluid. Considering Eqs. (1) and (2), the velocity distributions should not differ much from the first simulation, which can also be seen from Fig. 9. However, we illustrate the temperature distribution for this new working fluid in Fig. 8 and can find the patterns are mainly determined by fluid advection. At the beginning ($t = 0.004$ s), the isotherms close to the left side (hot source) are much more dense while the opposite situation occurs at $t = 0.016$ s. This is because the flow of high temperature from the hot source overwhelms and the equilibrium for this system tends to be that the high temperature occupies the whole area. If we exchange the positions of heat

and cold sources, the system would evolve to the situation that the temperature of the cold source occupies the whole area. Nevertheless, the cloak, concentrator, and rotator we design still work well in such a large Prandtl number.

For the simulation results of our gravity modeling shown in Figs. 9–11, we can still find that the differences of temperature, velocity, or heat flux are still small enough to be neglected. For liquids like water in our case, the influence of not transforming gravity $\vec{g}$ in our simulation would not violate the transformation theory significantly and it can still work well here in an approximate way. The same conclusion can also be obtained for mixed convection (namely, forced convection plus natural convection). It can be understood that for these cases, thermal conduction and forced convection (if any) are dominant, which can be seen from the patterns in Figs. 11–13. When the density of fluid changes more drastically, we must consider other methods to control heat flux in natural or mixed convection, such as various optimization techniques for controlling flows.[37–40]

On the other hand, the major difference between steady and unsteady cases is that the porosity and density (or specific heat) must be transformed as Eq. (7) for unsteady cases, which would be more complicated for experimental realization. We also perform similar simulations without changing ϕ or $\rho_s C_s$, and the resulting temperature distributions cannot be visually distinguishable with Fig. 2 or Fig. 11, which means that one can still use the steady-state material parameters for unsteady states in some cases where the temperature does not vary too fast.

In conclusion, we have developed the transformation theory for treating transient heat transfer with unsteady seepage flows in porous media and theoretically designed corresponding devices for thermal cloaking, concentrating, and rotating, respectively. In addition, we have introduced both the influence of natural/mixed convection in our model and the possibility to eliminate the difference of material parameters between steady and unsteady flows. We expect that this work could help us to promote the research on how to dynamically control heat transfer where thermal convection exists.

ACKNOWLEDGMENTS

We acknowledge the financial support by the National Natural Science Foundation of China under Grant No. 11725521 and by the Science and Technology Commission of Shanghai Municipality under Grant No. 16ZR1445100.

[1]C. Z. Fan, Y. Gao, and J. P. Huang, "Shaped graded materials with an apparent negative thermal conductivity," Appl. Phys. Lett. **92**, 251907 (2008).
[2]T. Chen, C. N. Weng, and J. S. Chen, "Cloak for curvilinearly anisotropic media in conduction," Appl. Phys. Lett. **93**, 114103 (2008).
[3]J. Y. Li, Y. Gao, and J. P. Huang, "A bifunctional cloak using transformation media," J. Appl. Phys. **108**, 074504 (2010).
[4]S. Guenneau, C. Amra, and D. Veynante, "Transformation thermodynamics: Cloaking and concentrating heat flux," Opt. Express **20**, 8207 (2012).
[5]S. Narayana and Y. Sato, "Heat flux manipulation with engineered thermal materials," Phys. Rev. Lett. **108**, 214303 (2012).
[6]R. Schittny, M. Kadic, S. Guenneau, and M. Wegener, "Experiments on transformation thermodynamics: Molding the flow of heat," Phys. Rev. Lett. **110**, 195901 (2013).
[7]H. Y. Xu, X. H. Shi, F. Gao, H. D. Sun, and B. L. Zhang, "Ultrathin three-dimensional thermal cloak," Phys. Rev. Lett. **112**, 054301 (2014).
[8]T. C. Han, X. Bai, D. L. Gao, J. T. L. Thong, B. W. Li, and C. W. Qiu, "Experimental demonstration of a bilayer thermal cloak," Phys. Rev. Lett. **112**, 054302 (2014).
[9]Y. G. Ma, Y. C. Liu, M. Raza, Y. D. Wang, and S. L. He, "Experimental demonstration of a multiphysics cloak: Manipulating heat flux and electric current simultaneously," Phys. Rev. Lett. **113**, 205501 (2014).
[10]T. Han, X. Bai, J. T. L. Thong, B. Li, and C. W. Qiu, "Full control and manipulation of heat signatures: Cloaking, camouflage and thermal metamaterials," Adv. Mater. **26**, 1731 (2014).
[11]K. P. Vemuri and P. R. Bandaru, "Anomalous refraction of heat flux in thermal metamaterials," Appl. Phys. Lett. **104**, 083901 (2014).
[12]T. Z. Yang, K. P. Vemuri, and P. R. Bandaru, "Experimental evidence for the bending of heat flux in a thermal metamaterial," Appl. Phys. Lett. **105**, 083908 (2014).
[13]T. Yang, X. Bai, D. Gao, L. Wu, B. Li, J. T. L. Thong, and C. W. Qiu, "Invisible sensors: Simultaneous sensing and camouflaging in multiphysical fields," Adv. Mater. **27**, 7752 (2015).
[14]Y. Li, X. Y. Shen, Z. H. Wu, J. Y. Huang, Y. X. Chen, Y. S. Ni, and J. P. Huang, "Temperature-dependent transformation thermotics: From switchable thermal cloaks to macroscopic thermal diodes," Phys. Rev. Lett. **115**, 195503 (2015).
[15]T. Y. Chen, C. N. Weng, and Y. L. Tsai, "Materials with constant anisotropic conductivity as a thermal cloak or concentrator," J. Appl. Phys. **117**, 054904 (2015).
[16]M. Raza, Y. C. Liu, and Y. G. Ma, "A multi-cloak bifunctional device," J. Appl. Phys. **117**, 024502 (2015).
[17]Y. Li, X. Y. Shen, J. P. Huang, and Y. S. Ni, "Temperature-dependent transformation thermotics for unsteady states: Switchable concentrator for transient heat flow," Phys. Lett. A **380**, 1641 (2016).
[18]X. Y. Shen, Y. Li, C. R. Jiang, and J. P. Huang, "Temperature trapping: Energy-free maintenance of constant temperatures as ambient temperature gradients change," Phys. Rev. Lett. **117**, 055501 (2016).
[19]Y. Li, X. Bai, T. Z. Yang, H. L. Luo, and C. W. Qiu, "Structured thermal surface for radiative camouflage," Nat. Commun. **9**, 273 (2018).
[20]R. Z. Wang, L. J. Xu, and J. P. Huang, "Thermal imitators with single directional invisibility," J. Appl. Phys. **122**, 215107 (2017).
[21]M. Maldovan, "Narrow low-frequency spectrum and heat management by thermocrystals," Phys. Rev. Lett. **110**, 025902 (2013).
[22]M. Maldovan, "Sound and heat revolutions in phononics," Nature **503**, 219 (2013).
[23]M. Maldovan, Phonon wave interference and thermal bandgap materials," Nat. Mater. **14**, 667 (2015).
[24]B. L. Davis and M. I. Hussein, "Nanophononic metamaterial: Thermal conductivity reduction by local resonance," Phys. Rev. Lett. **112**, 055505 (2014).
[25]S. Y. Xiong, K. Saaskilahti, Y. A. Kosevich, H. X. Han, D. Donadio, and S. Volz, "Blocking phonon transport by structural resonances in alloy-based nanophononic metamaterials leads to ultralow thermal conductivity," Phys. Rev. Lett. **117**, 025503 (2016).
[26]B. Li, K. T. Tan, and J. Christensen, "Tailoring the thermal conductivity in nanophononic metamaterials," Phys. Rev. B **95**, 144305 (2017).
[27]T. Zhu, K. Swaminathan-Gopalan, K. J. Cruse, K. Stephani, and E. Ertekin, "Vibrational energy transport in hybrid ordered/disordered nanocomposites: Hybridization and avoided crossings of localized and delocalized modes," Adv. Funct. Mater. **28**, 1706268 (2018).
[28]E. Rephaeli, A. Raman, and S. H. Fan, Ultrabroadband photonic structures to achieve high-performance daytime radiative cooling," Nano Lett. **13**, 1457 (2013).
[29]A. P. Raman, M. A. Anoma, L. X. Zhu, E. Rephaeli, and S. H. Fan, "Passive radiative cooling below ambient air temperature under direct sunlight," Nature **515**, 540 (2014).
[30]A. R. Gentle and G. B. Smith, A sub-ambient open roof surface under the mid-summer sun," Adv. Sci. **2**, 1500119 (2015).
[31]M. M. Hossain and M. Gu, "Radiative cooling: Principles, progress, and potentials," Adv. Sci. **3**, 1500360 (2016).
[32]N. N. Shi, C. C. Tsai, F. Camino, G. D. Bernard, N. F. Yu, and R. Wehner, "Keeping cool: Enhanced optical reflection and radiative heat dissipation in Saharan silver ants," Science **349**, 298 (2015).
[33]Y. Zhai, Y. G. Ma, S. N. David, D. L. Zhao, R. N. Lou, G. Tan, R. G. Yang, and X. B. Yin, "Scalable-manufactured randomized glass-polymer hybrid metamaterial for daytime radiative cooling," Science **355**, 1062 (2017).

[34]E. A. Goldstein, A. P. Raman, and S. H. Fan, "Sub-ambient non-evaporative fluid cooling with the sky," Nat. Energy **2**, 17143 (2017).
[35]S. Guenneau and T. M. Puvirajesinghe, "Fick's second law transformed: One path to cloaking in mass diffusion," J. R. Soc. Interface **10**, 20130106 (2013).
[36]S. Guenneau, D. Petiteau, M. Zerrad, C. Amra, and T. Puvirajesinghe, "Transformed Fourier and Fick equations for the control of heat and mass diffusion," AIP Adv. **5**, 053404 (2015).
[37]Y. A. Urzhumov and D. R. Smith, "Fluid flow control with transformation media," Phys. Rev. Lett. **107**, 074501 (2011).
[38]Y. A. Urzhumov and D. R. Smith, "Flow stabilization with active hydrodynamic cloaks," Phys. Rev. E **86**, 056313 (2012).
[39]P. T. Bowen, Y. A. Urzhumov, and D. R. Smith, "Wake control with permeable multilayer structures: The spherical symmetry case," Phys. Rev. E **92**, 063030 (2015).
[40]D. R. Culver, E. Dowell, D. R. Smith, Y. A. Urzhumov, and A. Varghese, "A volumetric approach to wake reduction: Design, optimization, and experimental verification," J. Fluids **2016**, 3587974 (2016).
[41]G. L. Dai, J. Shang, and J. P. Huang, "Theory of transformation thermal convection for creeping flow in porous media: Cloaking, concentrating, and camouflage," Phys. Rev. E **97**, 022129 (2018).
[42]COMSOL Multiphysics, Version 3.5, Burlington, MA, USA, 2008, see https://www.comsol.com/.
[43]J. B. Pendry, D. Schurig, and D. R. Smith, "Controlling electromagnetic fields," Science **312**, 1780 (2006).
[44]U. Leonhardt, "Optical conformal mapping," Science **312**, 1777 (2006).
[45]H. F. Burcharth and O. H. Andersen, "On the one-dimensional steady and unsteady porous flow equations," Coast Eng. **24**, 233 (1995).
[46]T. Zhu, C. Waluga, B. Wohlmuth, and M. Manhar, "A study of the time constant in unsteady porous media flow using direct numerical simulation," Transp. Porous Media **104**, 161 (2014).
[47]T. Zhu and M. Manhar, "Oscillatory Darcy flow in porous media," Transp. Porous Media **111**, 521 (2016).
[48]L. D. Landau and E. M. Lifshitz, *Fluid Mechanics*, 2nd ed. (Pergamon, London, 1987).
[49]J. Bear, *Dynamics of Fluids in Porous Media* (American Elsevier, New York, 1972).
[50]J. Bear and M. Y. Corapcioglu, *Fundamentals of Transport Phenomena in Porous Media* (Springer, 1984).
[51]M. Rahm, D. Schurig, D. A. Roberts, S. A. Cummer, D. R. Smith, and J. B. Pendry, "Design of electromagnetic cloaks and concentrators using form-invariant coordinate transformations of Maxwell's equations," Photonics Nanostruct. Fundam. Appl. **6**, 87 (2008).
[52]H. Chen and C. T. Chan, "Transformation media that rotate electromagnetic fields," Appl. Phys. Lett. **90**, 241105 (2007).